Paddy Water Environ (2006) 4: 39–51
DOI 10.1007/s10333-005-0028-0

ARTICLE

Julien Tournebize · Hirozumi Watanabe · Kazuhiro Takagi · Taku Nishimura

The development of a coupled model (PCPF-SWMS) to simulate water flow and pollutant transport in Japanese paddy fields

Received: 22 August 2005 / Accepted: 3 December 2005 / Published online: 10 February 2006

Abstract A new coupled model (PCPF–SWMS) was developed for simulating fate and behavior of pollutant in paddy water and paddy soil. The model coupled the PCPF-1, a lumped model simulating pesticide concentrations in paddy water and 1 cm-surface sediment compartment, and the SWMS-2D, a finite element numerical model solving Richard's and advection-dispersion equations for solute transport in soil compartment. The coupling involved improvements on interactions of the water flow and the concentration the pollutant of at the soil interface between both compartments. The monitoring data collected from experimental plots in Tsukuba, Japan in 1998 and 1999 were used to parameterise and calibrate hydraulic functioning, hydrodynamic and hydrodispersive parameters of the paddy soil. The analysis on the hydraulic functioning of paddy soil revealed that the hard pan layer was the key factor controlling percolation rate and tracer transport. Matric potential and tracer monitoring highlighted the evolution of saturated hydraulic conductivity (K_S) of hard pan layer during the crop season. K_S slightly decreased after puddling by clay clogging and strongly increased after mid term drainage by drying cracks. The model was able to calculate residential time in every soil layers. Residential time of tracer in top saturated layers was evaluated to be less than 40 days. It took 60 days to reach the unsaturated layers below hardpan layer.

Keywords Solute transport · Paddy soil · Paddy water · Tracer · Pesticide

J. Tournebize
CEMAGREF,
Parc de Tourvoie BP44,
92163 Antony, France

H. Watanabe · T. Nishimura
Tokyo University of Agriculture and Technology,
3-5-8, Saiwaicho, Fuchu, Tokyo 183-8509, Japan

K. Takagi (✉)
National Institute for Agro-Environmental Sciences,
3-1-3 Kannondai, Tsukuba 305-8604, Japan
e-mail: ktakagi@niaes.affrc.go.jp

Introduction

In Japan, paddy field system accounts for 55% of total arable land. Consequently, about a half of the total pesticide has been used for rice production in paddy fields. Japan is one of the top pesticide consumers in the world (IRRI 1991). As the paddy field functioning is different from the non-ponded crop cultivation, specific research is thus necessary. Pesticide use in rice cultivation generally takes place during the ponded period. The persistence of pesticides in paddy field affects the risk of aquatic pollution by two main ways: (i) through the surface runoff, (ii) through leaching in soil (Kibe et al. 2000). Forecasting hydraulic pathways and pollutant (nutrient and pesticide) behavior in paddy soil appear to be crucial in order to define the specific management practices controlling non-point source pollution and preserving water resources.

Many of simulation models for pollutant transport in paddy field concerned mainly surface water [e.g., PADDY, (Inao and Kitamura 1999), PCPF-1 (Watanabe and Takagi 2000a, b), RICEWQ, (Williams et al. 1999)]. As paddy soil presented stratified layers consisting of top puddled layer, hardpan layer, and underlying subsoil layer, the model simulation of acceptable water flow and pollutant transport has been considered difficult. Modeling study for ponded paddy field were generally based on deterministic approach (e.g., one-dimensional SAWAH model, (Wopereis et al. 1994), or three-dimensional FEMWATER model, (Lin et al. 1996)). Their main use was attributed to the water management, specially focused on percolation losses, water efficiency, and groundwater recharge (Wopereis et al. 1994; Bouman et al. 1994; Singh et al. 2001; Liu et al. 2001). In the models described by Tuong et al. (1994) and Liu et al. (2001), the liquid suspension on the top of the puddled layer was not included due to the no-flow resistance to vertical movement. Simulation results showed that water movement was mainly vertical percolation (compared to lateral flux) within a paddy field and that reduced percolation rate in the hardpan layer was the major factor controlling the infiltration rate (Chen et al. 2002). Indeed

hardpan layer complicates infiltration mechanisms by making it a variable saturated flow problem (Liu et al. 2001). In this circumstance, the parameter that primarily governs water percolation was the hydraulic conductivity of hardpan layer.

Modeling pollutant transport in both paddy water and paddy soil compartments has not been published until recently. Coupled models were developed and tested for nutrient management such as GLEAMS-PADDY (Chung et al. 2003), for a nitrogen and water balance model under flooded conditions (Chowdary et al. 2004). For pesticide transport in paddy soil, Miao et al. (2003) proposed an assimilated coupled model, RICEWQ-VADOFT. RICEWQ (Williams et al. 1999) simulates pesticide mass balance for surface compartment in rice field. VADOFT (Carsel et al. 1998) is an one-dimensional deterministic numerical model simulating solute transport in vadose zone solving Richard's equation in variably saturated porous media, and non-conservative chemical vertical transport. Nevertheless as mentioned by the authors, the models were not implicitly coupled; the output data of RICEWQ became the input data for VADOFT with no direct interaction between both.

In this context, we propose to develop a structurally coupled model between surface compartment and subsurface soil compartment for simulating pollutant fate and transport in paddy soil by combining two selected models, PCPF-1 (Watanabe and Takagi 2000a) and SWMS-2D (Simunek et al. 1994). PCPF-1 model, like PADDY or RICEWQ, is a lumped mass balance model which simulates concentration of pesticide in paddy water under different water management. SWMS-2D presented the modeling facility to be modified and incorporated the upper boundary condition needed in rice paddies. However, applicability to the ponded situation is unknown. Numerical simulation of heterogeneous layered soil in field-scale water flow and solute transport processes under ponded situation is a complex task even if hydraulic condition seems to be in apparent steady state. Such comprehensive modeling will help understand the mechanisms of pesticide fate and transport in paddy soil and it will serve as a platform for developing simpler models or generalized expression for evaluating environmental risks of the pesticides associated with rice production.

Hence, the specific objectives of the present paper are as follows: (1) Development of a coupled PCPF-1 and SWMS model to simulate the temporal dynamics of water flow and transport of tracer in rice fields under flooded conditions; (2) Assessment of hydraulic and transport parameters and validation of the model with a chloride (Cl^-) tracer from the experimental data.

Model description

PCPF-1

PCPF-1 (Pesticide Concentration in Paddy Field, version 1) is a lumped parameter model which simulates the pesticide fate and transport in two compartments, paddy water compartment and paddy surface-sediment layer compartment (Watanabe and Takagi 2000a). The paddy water compartment was assumed to be a completely mixed reactor having variable water depths. The surface-sediment compartment was defined as a 1 cm-thick conceptual surface paddy soil layer governing the pesticide dissipation and transport processes under oxidative flooded condition. The paddy soil layer was also assumed to be a completely mixed reactor with a constant depth. Both the compartments were assumed to be homogeneous, and having uniform and unsteady chemical concentrations.

The water balance of a paddy field was determined by irrigation supply, rainfall, surface runoff (overflow), evapotranspiration, lateral seepage, and vertical percolation. Pesticide concentrations in paddy water and surface sediment were calculated by considering the chemical fate processes such as pesticide adsorption, desorption, and degradation as well as dilution from irrigation and precipitation. Pesticide mass balance equations in paddy-water and surface-sediment compartments were iteratively solved for daily pesticide concentrations in corresponding compartments using fourth order Runge–Kutta method. Detailed description of the model was found in Watanabe and Takagi (2000a, b). PCPF-1 was validated and evaluated for common Japanese herbicides (Watanabe and Takagi 2000b; Watanabe et al. 2005a) and it was applied for the evaluation of water management practices in reducing pesticide runoff from Japanese paddy fields (Watanabe et al. 2005b).

For the pesticide transport through paddy soil, this surface-sediment layer served as a link between paddy water and lower puddled layer. The functions of oxidative surface sediment and reductive subsequent deeper soil layer were important since they exhibited different chemical fate phenomena (Chung et al. 2003). However, in this study, the model was modified and simplified for the case of non-reactive tracer without chemical processes described above.

SWMS-2D

SWMS-2D is the open source FORTRAN code of the commercial version "HYDRUS-2D" (Simunek et al. 1999), which is a Windows-based modeling environment for analysis of water flow and solute transport in variably saturated porous media. For further application concerning lateral water flow, we selected directly the 2D version instead of 1D. The program solves the Richards' equation for saturated–unsaturated water flow and a Fickian-based advection–dispersion equation for solute transport including provisions for linear equilibrium adsorption, zero-order production, and first-order degradation. The governing equations are solved using a Galerkin type linear finite element scheme. In this study, SWMS was utilized to simulate the flow of water and transport of chloride through the soil profile and to assess transport parameters. The

governing equations, without source or sink terms (in the case of tracer), are given by:

$$\frac{\partial \theta}{\partial t} = \frac{\partial}{\partial x_i} K(h) \left[\left(K_{ij} \frac{\partial h}{\partial x_i} + K_{iz} \right) \right] \quad (1)$$

$$\frac{\partial \theta c}{\partial t} = \frac{\partial}{\partial x_i} \left(\theta D_{ij} \frac{\partial c}{\partial x_j} \right) - \frac{\partial q_i c}{\partial x_i} \quad (2)$$

where θ is the volumetric water content ($cm^3\ cm^{-3}$), t is time (day), h is the water pressure head (cm), x_i is a spatial coordinate (cm), K_{ij} is a component of a dimensionless anisotropy tensor, and $K(h)$ is the unsaturated hydraulic conductivity function ($cm\ d^{-1}$). Subscripts i and j represent two directions, x (horizontal coordinate) and z (vertical coordinate), c is the solution concentration ($mg\ cm^{-3}$), D_{ij} is the dispersion coefficient tensor ($cm^2\ d^{-1}$), and q_i is the i-th component of the volumetric water flux ($cm\ d^{-1}$). D_{ij} is expressed as $D_{ij} = \lambda_T |q| \delta_{ij} + (\lambda_L - \lambda_T) q_j q_i / |q| + D^0 \tau \delta_{ij}$, with λ_T, λ_L, transverse and longitudinal dispersivity coefficient, respectively (cm), D^0, is the molecular diffusion coefficient in free water ($cm^2\ d^{-1}$), τ is a tortuosity factor, and δ_{if} is the Kronecker delta function. This expression is generally simplified as $D_{ii} = \lambda_L q_i$ and, $D_{jj} = \lambda_T q_j$.

PCPF–SWMS model

The model coupling was carried out by linking the percolation flux, induced by ponded water depth, and the predicted concentration at soil surface, at the interface between paddy-water compartment and paddy soil compartment using PCPF-1 and SWMS, respectively (Fig. 1).

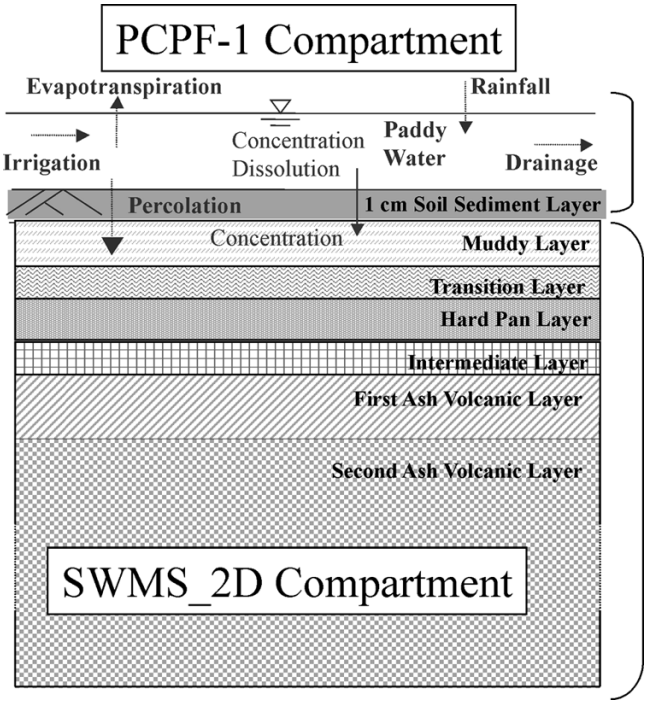

Fig. 1 Conceptual model compartment of PCPF-SWMS

Interaction between these two model compartments for water movement is described as follow: (i) PCPF-1 provides ponded water depth, considered as top boundary condition in SWMS (pressure prescribed data) and (ii) SWMS determines the daily vertical percolation rate, this value was involved in PCPF-1 water balance for the following day. We assumed that, when the paddy soil was always ponded, the effect of fluctuated ponded water depth was negligible on percolation rate. For the solute transport, the boundary condition at the interface between PCPF and SWMS was a third-type Cauchy boundary condition that prescribed the incoming solute flux. The solute flux was defined by the water percolation rate which is simulated by SMWS, and the dissolved tracer concentration which is simulated by PCPF.

Table 1 summarizes the input variables/parameters required by the PCPF–SWMS model. In addition, PCPF required daily climatic data: precipitation (cm), evapotranspiration (cm) during the simulated period. The evapotranspiration was calculated with Penman–Monteith equation following the FAO-56 method (Vu et al. 2005).

Materials and methods

Site location and agricultural practice

Field experiments were conducted at the experimental rice paddy field of National Institute for Agro-Environmental Sciences (NIAES) in Tsukuba, Japan (36°10′N, 139°56′E). The local average annual precipitation and temperature are 1406 mm and 14°C, respectively. Experiments were carried out in two of 9 m×9 m plots surrounded by concrete bunds and plastic borders in 1998 and 1999. The concrete block levees dividing experiments plots were covered by plastic sheets to prevent seepage across the plots. However, significant amount of vertical edge flow along the concrete borders and some leaks of paddy water through plastic sheets to the drainage basin were observed. Since those water paths were assumed to have negligible interaction with soil matrix, they were lumped with surface runoff.

Paddy plots were left fallow over the off crop season from October and plowed once in winter for controlling weeds. In April, plots were irrigated to puddle by two passes of rotary plow about 0.15 m deep, and leveled for the cultivation. General paddy field operation is also found in Adachi and Sasaki (1999). Seventeen-day-old rice seedlings (*Oryza sativa* L. cv. Nipponbare) were transplanted with 16 cm×30 cm spacing on May 8 in 1998, and on May 7 in 1999. The water-ponding condition was maintained until the mid-term drainage, starting July 17 in 1998 and July 16 in 1999, which was lasted for 17 and 10 days, respectively in 1998 and 1999. During the mid-term drainage, paddy water was drained and paddy soil was dried to promote agronomic conditions in the period from the maximum tillering stage to the panicle formation stage. During the reproductive stage after mid-term drainage, intermittent irrigation was performed until 1 week before the harvest (September 7, 1998, and September 27, 1999).

Table 1 Input parameters for modified PCPF-1 and SWMS

	Value 1998	Value 1999
PCPF-1		
Input parameters for paddy water		
Time interval (day)	1	
Tracer application rate (g m^{-2})	16	32
Paddy field area (m^2)	82.8	
Water depth at initial time (cm)	2.95	3.12
Pollutant concentration in irrigation water (mg l^{-1})	18	
Initial concentration (mg l^{-1})	256	486
Input parameters for pollutant source layer		
Depth (cm)	1	
Bulk density (g cm^{-3})	0.937	
Saturated volumetric water content (cm^3 cm^{-3})	0.603	
Initial concentration (mg kg^{-1})	25	
SWMS		
Input parameters for each layer in soil compartment		
Saturated water content (%)		
Residual water content (%)		
Van Genuchten parameter (α, n) (cm^{-1}, –)		
Saturated hydraulic conductivity (cm d^{-1})		
Bulk density (cm^3 kg^{-1})		
Longitudinal and transversal dispersivities (cm)		

All the dates for important events were summarized in Table 2. In this paper, those dates used were referred to as days after tracer application (DATA).

Soil properties and field monitoring

Table 3 shows physical and chemical properties of the soil of the NIAES experimental paddy plots. The material of upper 50 cm profile was brought from other site, and was covered by alluvial lowland soil during reclamation of the experimental plot about 30 years ago. The lower 50–125 cm deep layer was composed of original volcanic ash derived andisol, that characterized by extremely high organic matter content and low bulk density (Nanzyo et al. 1993).

Undisturbed soil core samples (5.1 cm high and 5.0 cm diameter) were collected at every layers with five replicates for obtaining soil water retention curves and saturated hydraulic conductivity curves. Soil water retention curves and soil parameters were determined by the method described in Klute (1986). The van Genuchten relationship of water retention (van Genuchten 1980) was obtained using the RETC optimization program (van Genuchten et al. 1991) by fixing saturated and residual water contents as measured values. Saturated hydraulic conductivities were determined by falling-head method. The analytical Mualem (1978) expression was used to describe the unsaturated hydraulic conductivity-water pressure head relationship.

In addition, bulk density and cone penetrometer data were measured *in situ* and in laboratory. The bulk density values were measured at every layers with five replicates. Cone penetrometer measurements were carried out every 5 cm from −5 to −40 cm deep.

A field monitoring was set up to observe the pressure head distribution in the soil profile of the experimental plots. A water depth sensor was installed to monitor the ponding water depth in each paddy plot. Two series of four tensiometers were inserted in the same plot along soil profile at −15, −30, −45, and −85 cm depth in 1998 and one series of the same tensiometers were installed at −10, −15, −45, and −85 cm depth in 1999. All data were acquired through data loggers. Data acquisition started after the tracer application, 0 DATA, until mid-term drainage, 66 DATA in 1998 and similarly until 63 DATA in 1999. We assumed that the depths of paddy surface layer and ponded water were uniform on all the surface of experimental plots. Note that, the monitoring data of matric potentials from 38 to 52 DATA in 1999 were not available due to technical troubles.

The inputs of KCl tracer were 1317 and 2633 g, for 1998 and 1999 corresponding to Cl^- ion tracer concentration of 256 and 486 mg l^{-1}, respectively. Paddy water was sampled every day during the first week, and weekly thereafter until mid-term drainage. In addition, two series of sintered glass porous cups were installed at −15, −30, −45, and −85 cm depth in 1998 and −15 and −45 cm in 1999 for soil water sampling. The soil water sampling was carried out by applying a vacuum of 500 cm (H_2O) continuously and sampled as weekly average about 500 ml. For the analysis of the chloride anion, a TOSOH ion-chromatography system equipped with an electric conductivity detector (CM-8020) was used. The column installed was an anion-exchange resin packed column (Shodex IC I-524A). The mobile phase was the aqueous solution containing 300 mM boric acid, 2.0 mM phthalic acid, and 1.84 mM tris(hydroxymethyl)aminomethane. The flow rate

Table 2 Agricultural practice and applied model with top boundary conditions

Year	1998			1999			Model	Top boundary condition for simulation
	Date	DATA	Monitoring	Date	DATA	Monitoring		
Continuous Irigation (Stage 1) 2–4 cm ponded water depth	4/21/1998	−21		4/20/1999	−24			
Transplant	5/8/1998	−4		5/7/1999	−7			
Tracer application	5/12/1998	0	T: 15, 30, 45, and 85 cm; Cpw; Cps: 15, 30, 45, 85 cm; PWD	5/14/1999	0	T: 10, 15, 45, 85 cm Cpw; Cps: 15, 45 cm; PWD	PCPF + SWMS	Time-dependent pressure head
Mid Term Drainage (Stage 2)	7/17/1998	66		7/16/1999	63		SWMS	Atmospheric boundary
Intermittent Irrigation (Stage 3) 0–5 cm ponded water depth	8/3/1998	83	Cps: 15, 30, 45, 85 cm; PWD	7/26/1999	73	Cps: 15, 45 cm; PWD	SWMS	Time-dependent pressure head
Final drainage	9/3/1998	114		9/23/1999	132			
Harvest	9/27/1998	138		9/30/1999	139			

DATA: day after tracer application, T: tensiometer; Cpw: sampling in paddy water, Cps: sampling in paddy soil with ceramic cup, PWD: ponding water depth.

of the mobile phase was 1.5 ml min^{-1}. The temperature of the column and detector were maintained at 40°C.

Model application

Whereas water potential measurements were conducted until the mid-term drainage, simulations were carried out from the 0 DATA until the final drainage before harvest (114 and 132 DATA for 1998 and 1999, respectively). The period of crop season was divided into three stages as indicated in Table 2: (i) stage 1 was the continuous ponding stage, period after the tracer application until the mid-term drainage (63 and 66 DATA in 1998 and 1999, respectively) for which the new coupled PCPF-SWMS simulation was performed; (ii) stage 2 covered the mid term drainage period, (64 to 83 DATA in 1998 and 67 to 73 DATA in 1999); (iii) stage 3 was the intermittent irrigation stage, period after mid term drainage until the final drainage before harvest. Stages 2 and 3 were simulated with nonmodified SWMS.

The grid space was set up at −1 cm from surface to −160 cm. Time discretization was set to be 1 day for PCPF-1 model. For SWMS, initial time step was 0.1 day, minimum and maximum time steps were 0.01 day and 1 day, respectively.

Boundary and initial conditions

For the PCPF–SWMS simulation of solute transport in NIAES experimental paddy field, the top boundary was set on the interface between the bottom of the 1 cm-surface-sediment layer and the top surface of puddled layer. The top boundary condition changed during simulation process according to the agricultural practices specified in Table 2. The coupled PCPF–SWMS model employed a time-dependent pressure head condition. The two other stages (running with nonmodified SWMS simulations) applied atmospheric conditions using daily atmospheric data as precipitation and soil evaporation (stage 2), and time-dependent pressure head conditions (stage 3). The bottom boundary was set for free-drainage (unit vertical hydraulic gradient) condition at the −160 cm from the top surface of puddled layer. No-flux boundary conditions were applied to the both sides of the flow domain. Third-type (or Cauchy type) boundary conditions was used to prescribe the solute concentration at the soil surface.

Initial conditions for matric potential were set in accordance with observations. Initial chloride concentrations for the whole domain were set up to background concentration to be 11 mg l^{-1} for the top surface layer and 25 mg l^{-1} for bottom layer. Besides, the concentration of irrigation water was fixed at the measured value of 11 mg l^{-1}.

During intermittent irrigation stage (stage 3), ponded water depth was strongly dependent of irrigation practice and percolation. Those hourly variations of ponded water depth could not be integrated in a daily timestep in this simulation model. In order to assess the performance of a daily timestep routine, a sensitivity analysis on percolation rate was

Table 3 Soil profile data of the experimental plot

	Layer					
	Muddy	Plow sole	Hard Pan calibrated	Transition	1st Volcanic Ash	2nd Volcanic Ash
Depth (cm)	0–17	17–21	21–23[a]	23–50	50–65	95–135
Texture	SCL	SCL		C	SiL	SiL
Coarse sand, 2.0–0.2 mm (%)		13.1		5.6	3.7	1.9
Fine sand, 0.2–0.02 mm (%)	46.7	34.8		29.6	36.2	27.3
Silt, 0.02–0.002 mm (%)	19.4	21.6		24.4	42.8	51.2
Clay, < 0.002 mm (%)	33.9	30.5		40.4	17.4	19.6
Total carbon content (%)	1.78	1.43		1.29	4.80	8.11
Total N content (%)	0.16	0.12		0.10	0.31	0.43
pH (H_2O)	5.20	6.38		6.54	6.54	5.62
pH (KCl)	4.1	5.10		5.23	5.23	4.83
Bulk density (kg/m^3)	1.28	1.43		1.36	0.70	0.57
Saturated water content (cm^3 cm^{-3})		0.438		0.475	0.709	0.717
α (cm^{-1})		0.0054		0.0047	0.005	0.0098
n		1.10		1.051	1.068	1.156
K_S measured (standard deviation) (cm d^{-1})	27 (23)	13.2 (5.5)		5.9 (4.3)	11.1 (9.5)	93 (82)
Calibrated K_S (cm d^{-1})	27	13.2	0.08[a]	4	8	10

K_S: saturated hydraulic conductivity

[a]Calibrated values

conducted by comparing with the result of hourly time step calculation. We ran hourly simulations with hourly measurements of ponded water depth of a short representative test period between 105 and 109 DATA. From an hourly irrigation input, a daily percolation rate, which was considered as reference (Perc(Ref)) was obtained. Then different constant ponding water depths (pwd = 0, 1, 2, 3, 5 cm) and observed daily minimum (pwd = d_{min}), daily maximum (pwd = d_{max}) and daily mean values (pwd = $d_{average}$) were examined. We calculated a daily cumulative percolation rate (Perc(pwd)). The daily cumulative simulated percolation flux (Perc(pwd)) was compared with the reference one (Perc(Ref)).

Parameter calibration and model evaluation

First, hydraulic parameters of the puddled layer (above hard pan layer) were fixed to their measured values given in Table 3. For hard pan layer, K_S was calibrated according to the observed pressure head profile of continuous ponding stage. For the second volcanic ash layer, K_S was estimated by applying the free drainage (unit gradient) condition associated with the measured matric potential at −85 cm depth.

For the solute transport parameters, D_{ii}=λq_i was estimated with known flow parameters and trial and error procedure for λ, using SWMS model in the forward mode by finding the best fit on the concentration front (rising parts) of the simulated and measured chloride breakthrough curves. Due to the high and variable background concentration, we used reduced concentration for the simplicity defined as followed:

$$C^* = \left(\frac{C - C_o}{C_{pulse} - C_o}\right)$$

where $C*$ is the relative concentration (dimensionless), C is the concentration of Chloride (mg l^{-1}), C_o is the initial or background concentration in the soil, and C_{pulse} is the equivalent concentration at the tracer pulse application (i.e., 256 mg l^{-1} in 1998 and 486 mg l^{-1} in 1999). During stage 3, K_S of hard pan layer was readjusted using the time series of chloride concentration, considering that dispersivity coefficient (calibrated in the previous step) was constant.

Results and discussion

Physical properties of paddy soil

The largest dry bulk density was 1.43 g cm^{-3} at 17–23 cm layer where the hard pan layer was located, while the smallest dry bulk density occurred at the depth of 85–125 cm with 0.57 g cm^{-3} in the original volcanic ash soil (Table 3). Also, the measured penetrometer value increased sharply with depth from the surface until the maximum value of 23 mm at −22.5 cm depth, and decreased in the non-puddled subsoil (Table 4). The measured K_S as well was greater at the surface layer (27 cm d^{-1}) and decreased with depth down to 5.9 cm d^{-1} at −25 cm in depth, and then increased gradually with depth until 93 cm d^{-1} at −85 cm deep layer (Table 3).

Bulk density profile indicated the development of a compacted layer at 17–23 cm in depth as showed by Aggarwal

Table 4 Average values (mm) and standard deviations (stdev in mm) of cone penetrometer measurements in soil profile above 40 cm

Depth (cm)	Average (mm)	Stdev (mm)
5	10.5	3.4
10	16.3	0.6
12.5	16.8	1.6
15	20.7	2.3
17.5	22.3	2.1
20	21.7	1.2
22.5	23.0	0.4
25	21.4	0.5
30	20.7	0.7
35	20.3	1.3
40	18.5	0.9

et al. (1995). The puddled layer changed gradually with depth into a more compact and denser layer. This suggested the formation of hard pan layer as discussed by Singh et al. (2001). This phenomenon was induced by puddling. Puddling broke soil aggregates, eliminated large soil pores, provoked compaction, clay dispersion, and clogging non-capillary pores responsible for greater water transmission through soils, and therefore, decreased K_S (Sharma and De Datta 1985; Tuong et al. 1994). Thus, determining precisely K_S of hard pan layer needed more investigation using numerical model described in next section.

As a first result, five distinct soil layers were defined for the model simulation (Table 3 and Fig. 1):

- Deep muddy layer (0–17 cm): a low water flow resistance layer (K_S=27 cm d^{-1}), characterized by a low dry bulk density (Wopereis et al. 1994).
- Deep transition layer (17–21 cm): a more compacted layer with a lower K_S (13.2 cm.d^{-1} between muddy layer and hard pan layer.
- Deep hard pan layer (21–23 cm): a layer exhibited very high flow resistance.
- Deep non-puddled transition subsoil layer (23–50 cm): a subsoil layer below hard pan layer, as shown by the penetrometer measurement.
- Deep layers (50–65 cm) and (65–135 cm): the original first and second volcanic ash soil layers.

Observed hydraulic and tracer concentration responses

Figures 2 and 3 showed evolution of measured matric potential from 0 to 63 and 66 DATA for 1998 and1999, respectively. For both monitoring years, in the top layers (0–20 cm in depth) tensiometer values were positive and fluctuated with small variations. Whereas in the subsurface layers, tensiometer values were negative. The matric potential at −85 cm in depth showed an unique tendency to decrease. This tendency revealed that the soil profile was reaching a new matric potential equilibrium after puddling and presaturation irrigation. In this case, the hydraulic state during continuous ponding stage was considered as a slow transient state in subsurface layers and depended on initial conditions and K_S value of hard pan layer. In 1998, matric potential showed the similar trend except for the −45 cm depth layer which exhibited two different decreasing slopes, before and after 45 DATA. This decrease in matric potential was reasonably attributed to a change in percolation rate as it is discussed in the next section. Comparing monitored values of 1998 and 1999, the inter-seasonal variations were low, indicating a seasonal reproducibility. Measured matric potential values were used to calibrate the model to determine the unknown K_S value during continuous ponding stage. Single K_S value was assigned for this stage in 1999, however, because of significant decline of measured matric potential during this stage in 1998, two K_S values were assigned for the period before and after 45 DATA.

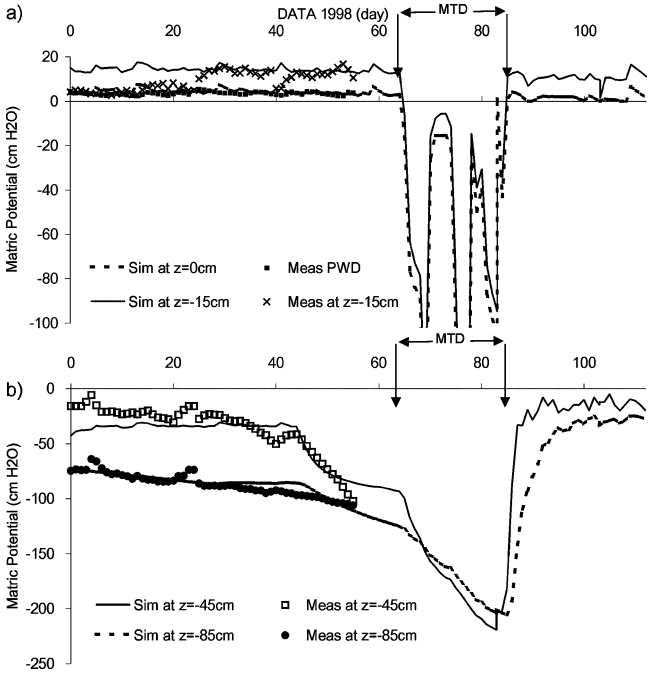

Fig. 2 Measured and simulated matric potentials and ponded water depths (PWD) versus day after tracer application (DATA), from May 13 to September 3, 1998; 0, −15 cm deep; (**a**) −45, −85 cm deep, (**b**) (MTD: mid-term drainage)

For the chloride concentration in paddy water, its peak was observed immediately after application, followed by a sharp decrease due to dilution and losses from irrigation and runoff during first 3 days after tracer application. After 10 DATA, concentrations in paddy water decreased as low as those of irrigation water. Figure 4 presents measured chloride concentrations for 1998 and 1999 in paddy soil. The maximum concentration at a depth of −15 cm occurred during the period of 25–35 DATA, and was higher in 1999 (52 mg l^{-1}) than in 1998 (23 mg l^{-1}) due to different application rates. For both monitored years, low concentrations were measured consecutively up to the mid drain drainage and somewhat increased again when intermittent irrigation stage started. Those phenomena were probably related to low water content in soil during suction sampling in the mid-term drainage. The peak amplitudes decreased with

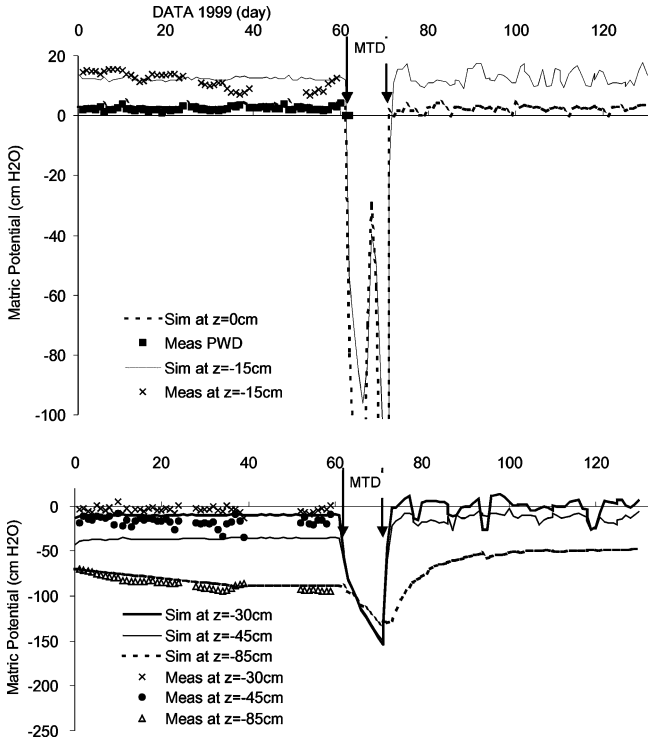

Fig. 3 Measured and simulated matric potentials and ponded water depths (PWD) versus day after tracer application (DATA), from May 5 to September 23, 1999; 0, −15 cm deep; (**a**) −30, −45, and −85 cm deep, (**b**) (MTD: Mid-term drainage)

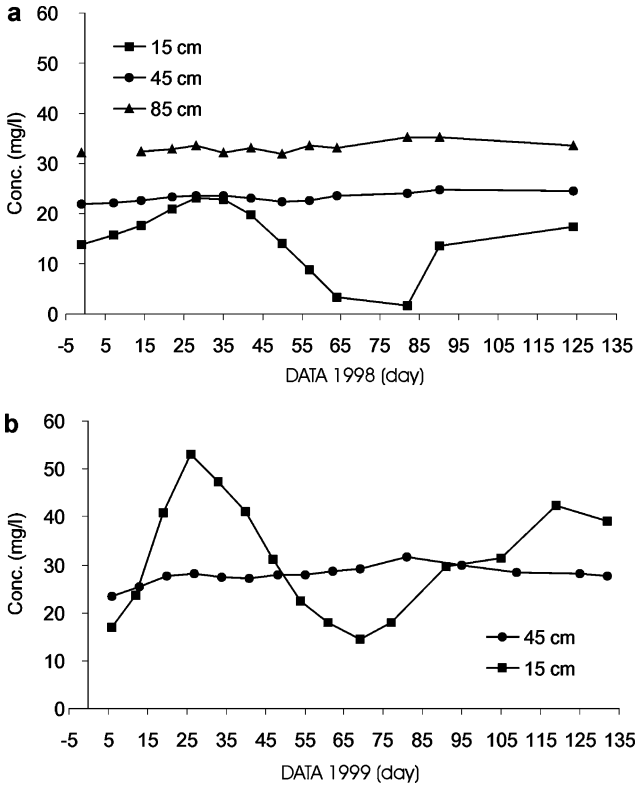

Fig. 4 Average observed chloride concentrations (mg l^{-1})... (**a**) at 15, 45 and 85 cm depth in 1998, and (**b**) at 15, 45 cm depth in 1999

depth, due to dilution, dispersion, and partially to higher background concentration of 15, 22, and 32 mg l^{-1} at −15, −45 and −85 cm deep layer, respectively. At −45 cm in depth, a small peak could be distinguished during the period of 85–95 DATA. Solute transport phenomena in soil profile was analyzed with reduced concentration. Nevertheless, the choice of chloride as tracer was considered to be inappropriate for higher back ground concentration.

PCPF-SWMS model simulation

Continuous ponding stage

Hydraulic parameters determination Measured matric potential profiles of the 2 years were compared with predicted values using calibrated parameters in Fig. 5. The simulated and observed pressure head distributions for both years were almost identical. The shape of the curves in Fig. 5 was similar to the observations reported by Adachi and Sasaki (1999) and Wopereis et al. (1994). In puddled layer, the soil-water pressure head increased linearly with depth with a slope close to the unit gradient until −17 cm in depth. This relationship confirmed that the puddled layer did not impose any substantial resistance to water flow (Chen and Liu 2002). The pressure head started decreaseing thereafter. In the layer with more compacted and dense profile, the pressure head decreased rapidly and became negative from the middle of the hard pan layer, generating a high hydraulic gradient. Numerical resolution instabilities, originated from this abrupt hydraulic gradient, were solved by decreasing time step and refining the finite element mesh. In the unsaturated zone, the pressure head decreased according to the properties of each layer until the measured value of about −85 cm H_2O, which is imposed by the unit gradient bottom boundary condition. This relatively high value of pressure head for an unsaturated soil corresponded to more than 90% saturation (99% saturation in transitional layer, 98% saturation in first ash volcanic layer, and 90% saturation in second ash volcanic layer). This suggested that as water between soil particles was linked, vertical water movement in this region was dominated by gravitational flow, highlighting the similar potential risk of tracer movement as in the saturated condition.

The optimized K_S of subsoil were 4, 8, and 10 cm d^{-1} for the layer of [−23; −50 cm], [−50; −65 cm] and [−65; −160 cm], respectively. All the optimized values were within the range of measurements: 1.6 and 10.2 cm d^{-1} for [−23; −50 cm] layer, 1.6 and 20.6 cm d^{-1} for [−50; −65 cm] layer, and 11 and 175 cm d^{-1} for [−65; −160 cm] layer, respectively. The difference between measured and optimized K_S for deeper layers was mainly due to a high variability of measurement and to soil characteristics of the volcanic ash soil. The K_S value of the hard pan layer was optimized to be 0.08 cm d^{-1}. This value was very low compared with other layers, however, it was in accordance with values such as 0.03 and 0.05 cm d^{-1} found by Bouman et al. (1994) and Chen and Liu (2002), respectively. The re-

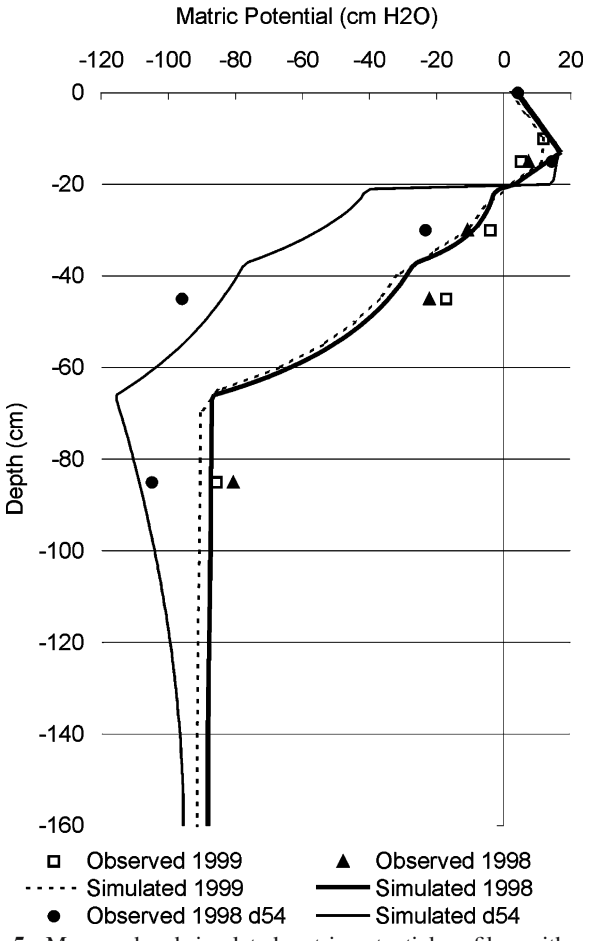

Fig. 5 Measured and simulated matric potential profiles, with optimized on K_S in 1998 and 1999, and with a new optimized K_S for the DATA = 54 day in 1998

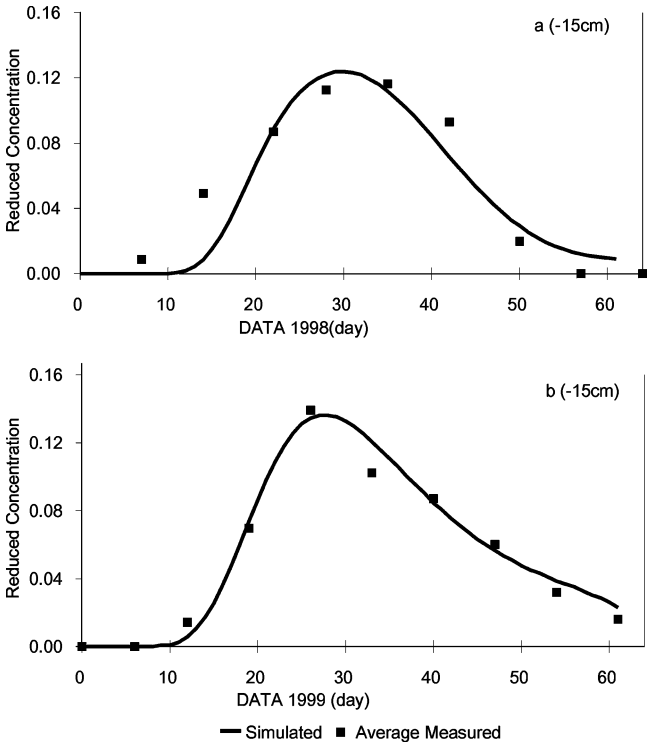

Fig. 6 Average measured and simulated concentrations at −15 cm deep versus day after tracer application (DATA); **a** from May 13 to July 7, 1998, **b** from May 15 to July 12, 1999

sults of Wopereis et al. (1994) indicated that infiltration rate reduced in the order of 50 to 1000 times due to puddling effect.

As mentioned in the previous section, measured pressure heads at the depth of −45 cm in 1998 changed during continuous ponding period. Therefore, a new optimized K_S of 0.04 cm d^{-1} was set for the period after 40 DATA to fit the corresponding matric potential profile. Including both the optimized K_S of hard pan layer, the model reproduced satisfactorily the entire matric potential evolution of every layers (Figs. 2 and 3). This result also proved that the evolution of the hard pan layer depending on puddling and ponded conditions. Indeed this reduction in K_S of the hard pan layer should be due to fine particle sealed clay translocation, which gradually reduced percolation rate. The evolution of hydraulic properties of hard pan layer distinctly influenced the percolation rate.

Simulated water flow and tracer concentration For the water balance components, the percolation rate was directly calculated from Darcy law in the SWMS code. The simulated percolation rate of paddy soil profile depended strongly on K_S of the least permeable layer such as the hard pan layer. The average simulated percolation rate for the period from 1 to 44 DATA and from 45 to 65 DATA in 1998 were 0.24 and 0.084 cm d^{-1}, respectively. For the period from 1 to 63 DATA in 1999, the percolation rate was 0.24 cm d^{-1}. Fluctuations of percolation rate vary from 0.22 to 0.26 cm d^{-1}, showing that the percolation rate was slightly sensitive to ponded water depth. Those values were in accordance with the average percolation rate (0.2 cm d^{-1}) in previous studies of Watanabe and Takagi (2000b). Comparing with single PCPF-1 model (Watanabe and Takagi 2000b), the new coupled model was able to adjust percolation rate according to ponded water depth and hydraulic properties.

The tracer concentration was simultaneously and accurately simulated by the PCPF-SWMS model (Fig. 6). The accurate estimation of the top boundary concentration condition was crucial to quantify the amount of applied tracer entering the soil profile.

The longitudinal dispersivity coefficient was fitted by try and error procedure for the continuous ponding period up to 60 DATA for 1998. Considering the high variability of natural paddy soil water concentration, simulated results with longitudinal dispersivity of 1 cm were considered to be in a good agreement with measurement data. Finally, the time to peak for the tracer concentration at the depth of −15 cm was simulated for 30 DATA for both 1998 and 1999, and compared with observed values ranged between 27 and 31 day. At the end of the continuous ponding stage, the simulated tracer front was located between 27 and 29 cm

in depth. This implied that the tracer needed at least 63 days to travel from the top to the bottom of hard pan layer.

Midterm drainage stage

As explained previously, as PCPF-1 is not able to simulate the non-ponding condition, the water flow and the tracer concentration in paddy soil in midterm drainage and intermittent irrigation stages were simulated using SWMS-2D only. During the mid term drainage as ponding water was drained, soil surface was then subject to natural climatic conditions such as evapotranspiration and precipitation. Hence, simulated soil matric potentials fluctuated according to those conditions. Due to the greater rainfall amount in 1999 from 80 DATA, the lowest pressure head in topsoil was only up to −160 cm H_2O, whereas in 1998 (drier period), the lowest pressure head in the top layer was below −1000 cm H_2O. Deeper in subsoil, matric potential showed less effects from the variations in the top layer.

The changes in soil structure and properties, especially cracks generated during the drying process were ignored in the simulation. According to previous studies (Kirby and Ringrose-Voase 2000; Mohanty et al. 2004; Liu et al. 2004), the crack development was within −10 to −15 cm depth for about one to two weeks after the start of mid-term drainage. Besides, Kukal and Aggarwal (2003) measured that 97% of root mass remained in the top 20 cm layer in a well-puddled soil due to the hardly-penetrated compacted layer. Therefore, we reasonably assumed that drying cracks and macropores generated by roots remained in the upper layer, i.e. in the puddled layer and top of the hard pan layer. In addition, simulation showed that during continuous ponding stage, the tracer reached the bottom of the hard pan layer. As the water flow in top soil layers was influenced mainly by evapotranspiration, we assumed that the effects of the water movement on the tracer transport was negligible. Thus, the tracer was treated presumably immobile in all soil profile during this stage.

Intermittent irrigation stage

The results of the sensitivity analysis on fluctuating ponded water depth were summarized in Table 5. The relative error (%) between the cumulated percolation volume at indicated ponded water depth (Perc(pwd)) and the cumulated percolation volume at hourly simulated ponded water depth (Perc(Ref) as reference at different soil layers. When the value was positive, the ponded water boundary condition overestimated the reference value, otherwise underestimated it.

The sensitivity analysis revealed two different aspects. Firstly, the results indicated that for all situations, the top layers (above the bottom of hard pan layer, >−23 cm) were more sensitive than the bottom layers (below hard pan layer) for changing water depth. The effects of the variations of the top boundary condition diminished with depth. Secondly, the daily time step simulation with a daily mean percolation that calculated from hourly water depth per day gave numerical stability and the less error, which is below 2% difference from hourly time step simulation. Solution convergence using SWMS was better with daily variable water depth (pwd = $d_{average}$) than with constant ponded water depth (pwd = mean). Hence, sensitivity analysis revealed that a constant pressure head condition for the whole period was not as suitable as a daily calculated value. It also confirmed that the percolation rate in this intermittent irrigation period was slightly sensitive to the ponded water depth. Anbumozhi et al. (1998) reported that the change in ponded water depth was not substantial from 1 to 9–10 cm for percolation rate whereas Bouman et al. (1994) found the contrary results. Physically, the very low K_S of the hard pan layer generated a large hydraulic gradient across the semi-impermeable hard pan layer (depending on its thickness) which was responsible of the percolation rate variations. Sensitivity of ponded water depth was linked to saturated hydraulic conductivity and to the thickness of hard pan layer.

As mid term drainage modified the properties of top-soil layer, a new set of K_S parameters was determined for the intermittent irrigation stage. Because of the lack of tensiometer measurements, calibration of hydraulic parameters using matric potential was not possible. Thus, the hydraulic functioning during this stage was estimated only with tracer data. The value of the longitudinal dispersivity (λ=1 cm) was assumed to remain the same for all layers and for the full crop season. The saturated hydraulic conductivity of hard pan layer was reset in order to fit the tracer peak. At a depth of −45 cm, the observed peak concentra-

Table 5 Sensitive analysis with relative errors on flux for daily simulation in comparison using hourly simulation as reference (Perc(ref)), with constant ponded water depth (Perc(pwd)

pwd = 0, 1, 2 cm or, pwd = mean(=2.2), 3, 5 cm) and with constant daily maximum (pwd = d_{max}), minimum (pwd = d_{min}) and constant daily average (pwd = $d_{average}$)

	Relative error (%) for various depth in soil profile (cm)						
Pwd (cm)/soil depth (cm)	−1	−7	−14	−23	−39	−68	−160
0	−10%	−10%	−10%	−11%	1%	0%	−1%
1	−5%	−5%	−5%	−3%	−2%	−1%	0%
2	−1%	−1%	−1%	1%	0%	0%	0%
2.2	1%	1%	1%	2%	1%	1%	0%
3	4%	4%	4%	4%	3%	2%	0%
5	17%	17%	17%	11%	5%	2%	0%
d_{max}	16%	16%	16%	3%	1%	1%	1%
$d_{average}$	0%	0%	0%	1%	−1%	−2%	−1%
d_{min}	−9%	−9%	−9%	−9%	−1%	−1%	−1%

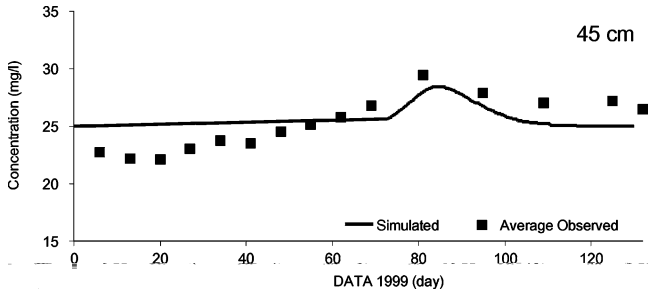

Fig. 7 Simulated and average observed Cl^- concentrations at −45 cm depth versus DATA in 1999

tions occurred around 90 DATA in 1998 and between 81 and 90 DATA in1999, respectively. Figure 7 showed simulated and measured concentrations at −45 cm depth layer including background concentration. As compared with the values of continuous ponding stage, the new optimized K_S significantly increased from 0.04 to 0.8 cm d^{-1} after the midterm drainage for 1998 and from 0.08 to 0.3 cm d^{-1} for 1999, respectively. Below hard pan layer, pressure heads were −10 cm H_2O at −45 cm in depth and −80 cm H_2O at −85 cm in depth, which were higher than stage 1. This new steady state hydraulic profile was mainly caused by higher percolation rate induced by higher K_S of top layer presumably due to drying cracks and rice root development after mid term drainage. Those results agreed with previous studies (Tuong et al. 1994; Liu et al. 2004) which showed that a small break in hard pan layer was sufficient to increase percolation rate 10 times. Because the mid term drainage was longer in 1998 (17 days), and drying cracks was assumed to develop more in the soil, the K_S of hardpan layer was higher in 1998 (0.8 cm d^{-1}) as compared to 1999 (0.3 cm d^{-1}).

Tracer movement during crop season

Once hydraulic functioning was set up, the model was able to simulate the tracer residential time in every layers with good accuracy. The simulation of tracer movement by PCPF-SWMS forecasted the residential time in paddy water and surface sediment layer of about 15 and 10 days in 1998 and 1999 under prescribed water management. The chloride leachate through paddy surface sediment layer was estimated to be 5.4% of applied mass for both years. The residential period at the bottom of puddled layer (1–17 cm) started from 11 to 9 DATA for 1998 and 1999, respectively, and lasted until 60 and 50 DATA for 1998 and 1999, respectively. The peak concentrations then occurred at 26 and 23 DATA (Fig. 6). The residential period for the tracer in the hard pan layer was simulated from 21 to 85 DATA with a peak at 42-40 DATA. Tracer was simulated to reach at the −67 cm depth, the area with a unit gradient (Fig. 5), at least after 95 DATA with an expected peak lay between 107 and 121 DATA. Figure 8 shows tracer concentration profiles at 63 and 66 DATA in 1998 and 1999, respectively during mid-term drainage stage and one before the harvest at 112 and 131 DATAfor 1998 and 1999, respectively.

The hydraulic profile of 0 to −160 cm in depth which was near saturation, provided the favorable condition for the tracer migration.

Conclusions

A lumped parameter model simulating pesticide concentration in paddy field, PCPF-1 and two-dimensional model for solute transport in soil, SWMS-2D were coupled as a Fortran code of PCPF-SWMS. Hydraulic and solute transport parameters were calibrated with monitored field data of Japanese paddy field.

Simulation of water and tracer movements for the entire crop season using fitted parameters drew following conclusions. The analysis on the hydraulic functioning of paddy soil revealed that the hardpan layer was the key factor controlling percolation rate and tracer transport. The pressure heads evolution during the monitoring period agreed well with those observed. The hard pan layer, which had the lowest hydraulic conductivity in the profile, retained the infiltrating water within the puddled layer and remained saturated, by such water management. Percolation rates in-

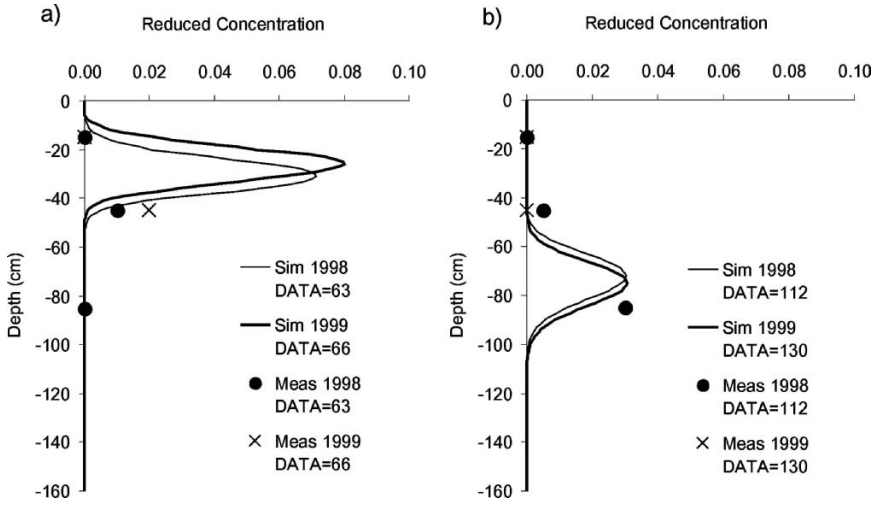

Fig. 8 Simulated and measured tracer concentration (reduced concentration) profiles in soil in 1998 and 1999 at two different dates; **a** before mid term drainage and **b** at the end of simulation before harvest drainage

creased after mid-term drainage probably because drying cracks and root penetration generated in the hard pan layer during mid-term drainage. Evolution of percolation rate should be embedded for tracer leachate during entire crop season. Residential time of tracer in top saturated layers was evaluated to be less than 40 days. It took 60 days for the tracer to reach the unsaturated layers below hardpan layer. However, the subsoil layer below hardpan was near saturation, which presented favorable conditions for pollutant transport to neighboring aquatic environments and poses environmental risks associated with rice production in Japan.

Acknowledgements The authors thank different institutions Tokyo University of Agriculture and Technology, National Institute for Agro-Environmental Sciences of Japan and Cemagref of France for their benevolence. This research was funded by the Innovative Technology Research Project in the Ministry of Agriculture, Forestry and Fisheries and partially supported by a Domestic Research Fellowship from Japan Science Technology Corporation and JAPAN- FRANCE integrated action program SAKURA by the Japan Society for the Promotion of Science (JSPS, number 1522) and the Ministere des Affaires Etrangères in France (MAE number 06986). The authors thank the reviewers and Dr Manon Janssen for their comments.

References

Adachi K, Sasaki C (1999) Percolation and seepage, In: Miztani M.: Hasegawa S., Koga K., Goto A., Murty V.V.N. (eds) Advanced paddy field engineering. JSIDRE, pp 72–88

Aggarwal GC, Sidhu AS, Sekhon NK, Sandhu KS, Sur HS (1995) Puddling and N management effects on crop response in a rice-wheat cropping system. Soil Till Res 36:129–139

Anbumozhi V, Yamaji E, Tabuchi T (1998) Rice crop growth and yield as influenced by changes in ponding water depth, water regime and fertigation level. Agric Water Manage 37:241–253

Bouman BAM, Wopereis MCS, Kropff MJ, Tenberge HFM, Tuong TP (1994) Water-use efficiency of flooded rice fields .2. Percolation and seepage losses. Agric Water Manage 26:291–304

Carsel RF, Imhoff JC, Hummel PR, Cheplick MJ, Donigian AS (1998) PRZM-3, a model for predicting pesticide and nitrogen fate in the crop root and unsaturated soil zones. Users manual for release 3.0

Chen S-K, Liu CW, Huang H-C (2002) Analysis of water movement in paddy rice fields (II) simulation studies. J Hydrol 268:259–271

Chen S-K, Liu CW (2002) Analysis of water movement in paddy rice fields (I) experimental studies. J Hydrolo 260:206–215

Chowdary VM, Rao NH, Sarma PBS (2004) A coupled soil water and nitrogen balance model for flooded rice fields in India. Agric Ecosyst; Environ 103(3):425–441

Chung SO, Kim HS, Kim JS (2003) Model development for nutrient loading from paddy rice fields. Agric Water Manage 62:1–17

Inao K, Kitamura Y (1999) Pesticide paddy field model (PADDY) for predicting pesticide concentrations in water and soil in paddy fields. Pestic Sci 55:38–46

IRRI (1991) Land use, irrigation, and farm size. World Rice Statistics 1990. Internation Rice Research Institute, Laguna Philippines, pp 201–221

Kibe K, Takahashi M, Kameya T, Urano K (2000) Adsorption equilibriums of principal herbicides on paddy soils in Japan. Sci Environ 263:115–125

Kirby JM, Ringrose-Voase AJ (2000) Drying of some Philippine and Indonesian puddled rice soils following surface drainage: numerical analysis using a swelling soil flow model. Soil Till Res 57:13–30

Klute A (1986) Methods of Soil Analysis. In: Klute A (ed)

Kukal SS, Aggarwal GC (2003) Puddling depth and intensity effects in rice-wheat system on a sandy loam soil I. Development of subsurface compaction. Soil Till Res 72:1–8

Lin HC, Richards DR, Yeh GT, Cheng JR, Cheng HP, Jones NL (1996) FEMWATER: a three-dimensional finite element computer model for simulating density dependent flow and transport. Tech Rep

Liu CW, Chen SK, Jou SW, Kuo SF (2001) Estimation of the infiltration rate of a paddy field in Yun-Lin, Taiwan. Agric Syst 68:41–54

Liu CW, Chen SK, Jang CS (2004) Modelling water infiltration in cracked paddy field soil. Hydrol Processes 18:2503–2513

Miao ZW, Cheplick MJ, Williams MW, Trevisan M, Padovani L, Gennari M, Ferrero A, Vidotto F, Capri E (2003) Simulating pesticide leaching and runoff in rice paddies with the RICEWQ-VADOFT model. J Environ Qual 32:2189–2199

Mohanty M, Painuli DK, Mandal KG (2004) Effect of puddling intensity on temporal variation in soil physical conditions and yield of rice (*Oryza sativa* L.) in a Vertisol of central India. Soil Till Res 76:83–94

Mualem Y (1978) Hydraulic conductivity of unsaturated porous media: generalized macroscopic approach. Water Resour Res 14:325–334

Nanzyo M, Shoji S, Dahlgren R (1993) Physical characterictics of volcanic ash soils, In: Development in soil science, vol 21, Volcanic ash soils genesis, Properties and utilization. Elsevier, Amsterdam, pp 189–208

Sharma PK, De Datta SK (1985) Effects of puddling on soil physical properties and processes. In: IRRI (ed) Soil physics and rice, Los Banos, Philippines, pp 217–234

Simunek J, Vogel T, van Genuchten MTh (1994) The SWMS_2D Code for simulating water flow and solute transport in tow dimensional variably saturated media (Version 1.21). Research Report No. 132. US Salinity Laboratory Agricultural Research Service, US Department of Agriculture, Riverside, California

Simunek J, Sejna MT, van Genuchten M (1999) The Hydrus-2D Software Package for Simulating the Two-dimensional Movement of Water, Heat, and Multiple Solutes in Variably Saturated Medai, Version 2.0. IGWMC-TPS-70, International Ground Water Modeling Center, Colorado School of Mines, Golden Colorado

Singh KB, Gajri PR, Arora VK (2001) Modelling the effects of soil and water management practices on the water balance and performance of rice. Agric Water Manage 49:77–95

Tuong TP, Wopereis MCS, Marquez JA, Kropff MJ (1994) Mechanisms and control of percolation losses in irrigated puddled rice fields. Soil Sci Soc Am J 58:1794–1803

van Genuchten M (1980) A closed-form equation for predicting the hydraulic properties of unsaturated soils. Soil Sci Soc Am J 49:1093–1099

van Genuchten M, Leij FJ, Yates SR (1991) The RETC code for quantifying hydraulic functions of unsaturated soils. US Salinity Laboratory, US Department of Agriculture, ARS, Riverside

Vu SH, Watanabe H, Takagi K (2005) Application of FAO-56 for evaluating evapotranspiration in simulation of pollutant runoff from paddy rice field in Japan. Agric Water Manage 76(3):195–210

Watanabe H, Takagi K (2000a) A simulation model for predicting pesticide concentrations in paddy water and surface soil. I. Model development. Environ Technol 21:1379–1391

Watanabe H, Takagi K (2000b) A simulation model for predicting pesticide concentrations in paddy water and surface soil II. Model validation and application. Environ Technol 21:1393–1404

Watanabe H, Takagi K, Vu SH (2005a) Simulation of mefenacet concentrations in paddy field by improved PCPF-1 model. Pest Manage Sci (in press)

Watanabe H, Vu SH, Tournebize J, Nguyen MHT, Komany S, Phong TK, Hien TQ, Ishihara S, Takagi K (2005b) Monitoring and Modeling of Pesticide Fate and Transport in Paddy Fields; Challenges for Reducing Environmental Risk. Proceedings of the 2nd International Conference of Japan Korea Research Cooperation, Impact Assessment of Farm Chemicals Runoff from Paddy Field and Biodiversity Conservation. March 16, 2005. Tsukuba, Japan. pp 69–82

Williams MW, Ritter AM, Cheplick MJ, Zdinak CE (1999) RICEWQ: Pesticide runoff model for rice crops. Users manual and program documentation. Version 1.6.1

Wopereis MCS, Bouman BAM, Kropff MJ, Tenberge HFM, Maligaya AR (1994) Water-use efficiency of flooded rice fields .1. Validation of the soil-water balance model sawah. Agric Water Manage 26:277–289